CHEMISTRY
AN ASIAN JOURNAL
www.chemasianj.org

Accepted Article

Title: Construction of a Luminogen Exhibiting High Contrast and Multicolored Emission Switching through Combination of a Bulky Conjugation Core and Toly Groups

Authors: Yong Qiang Dong, Yuxin Duan, Huili Ma, Haiyan Tian, Jing Liu, Xuebin Deng, and Qian Peng

To be cited as: *Chem. Asian J.* 10.1002/asia.201801608

Link to VoR: http://dx.doi.org/10.1002/asia.201801608

A Journal of
ACES
Asian Chemical Editorial Society

A sister journal of **Angewandte Chemie** and **Chemistry – A European Journal**

WILEY-VCH

Construction of a Luminogen Exhibiting High Contrast and Multicolored Emission Switching through Combination of a Bulky Conjugation Core and Tolyl Groups

Yuxin Duan, [a] Huili Ma, [b] Haiyan Tian, [a] Jing Liu, [a] Xuebin Deng, [a] Qian Peng, *[b] and Yong Qiang Dong,* [a]

Dedication ((optional))

Abstract: Stimuli responsive luminogens may find application in highly sensitive sensors, memories and security inks. However, few examples exhibiting both high contrast and multi-colored emission switching have been reported due to the absence of molecular design strategy. Through combination of large conjugation core and peripheral phenyl rings, we obtained ditolyldibenzofulvene (**1**). Luminogen **1** is AIE active and exhibits tetracolored emission depending on its morphology. Its three single crystals emit blue, yellow and dark orange light upon excitation, exhibiting a maximal emission of 461 nm, 545 nm and 586 nm, respectively, and its amorphous solid emits at 557 nm. All the four aggregates exhibit enhanced emission intensity at lower temperature, but only the orange emissive crystals exhibit blue-shifted emission. The emission of **1** can be switched reversibly between any two of the four states through morphology tuning. Finally, the potential application of **1** in optical data storage was also investigated.

Introduction

Stimuli responsive luminescent materials have drawn much attention due to their potential applications in sensors, memories and security inks fields.[1] Of particular interest are those exhibiting mechanochromic (MC), solvochromic, thermochromic emission in the solid state.[2] Some luminogens, including liquid crystals,[3] organic molecules,[4] organometallic compounds,[5] polymers or dye-doped polymers,[6] exhibit morphology dependent emission and their emission can be switched through morphology tuning. However, luminogens exhibiting MC emission switching had been rare as many panel-like luminogens experience aggregation caused quenching (ACQ) in the solid state.[2b, 7] A group of propeller-like luminogens are nonemissive in solution, but emit brightly in aggregate states, which is coined as aggregation induced emission (AIE) by Tang and coworkers.[8] In addition, many AIE luminogens (AIEgens) exhibit enhanced emission intensity and blue-shifted PL spectra upon crystallization, which is coined as crystallization induced emission enhancement (CIEE).[1c, 9] The twisted conformations afford loose packing patterns, which facilitates the transformation of AIEgens between amorphous and crystalline states upon exposure to external stimuli. Thus, emissions of many AIEgens can be switched among two states through modulating morphology of the luminogen between amorphous and crystalline states.[3, 10]

However, MC luminogens exhibiting multicolored or high contrast emission switching, are rather rare due to lack of design strategy, in spite of their potential to improving anti-fake complexity and density of optical storage.[11] Some serendipitous examples exhibiting tricolored emission switching have been reported including liquid crystal mixture with 9,10-bis(phenylethynyl)anthracene by Sagara and Kato,[3] twisted donor acceptor type MC luminogen by Ma and coworkers,[12] tetraphenylethylene linked rhodamine B by Jia and coworkers,[13] and so forth. Chi and coworkers reported one tetraphenylethene derivative with 6-hydroxylbenzothiazole, whose emission can be tuned among four colors through mechanical stimulus protonation and deprotonation, while the chemical structure is changed upon protonation.[14] Sagara and Weder achieved modulation of one cyano-substituted oligo(p-phenylene vinylene) among five emissive states.[15] However, it is a pity that reversible switching cannot be achieved between some states in the both systems developed by Chi and Sagara.

In addition to aforementioned progress of MC luminogens with multicolored emission, we noticed that some luminogens cored with twisted AIEgens exhibit multicolored MC luminescence due to the synergism of twisted conformation and weak intermolecular interaction.[11a] Furthermore, luminogens constructed by combination of large conjugation core and peripheral phenyl rings may exhibit high contrast MC luminescence[16], while reversible switching among all the morphologies was not achieved. In this paper, we replaced alkoxy phenyl groups with tolyl groups, and synthesized ditolyldibenzofulvene (DTDBF, **1**) with twisted conformation, a bulky conjugation core and peripheral tolyl groups. Modification of molecular structure will affect the molecular packing patterns and intermolecular interaction, thus, luminogen **1** exhibits tetracolored emission depending on its morphology, and three single crystals with blue, yellow and dark orange emission were obtained, which exhibits a maximal emission of 461 nm, 545 nm and 586 nm, respectively, and its amorphous solid emits at 557

---

[a] Y. Duan, H. Tian, J. Liu, Prof. Y. Dong
Beijing Key Laboratory of Energy Conversion and Storage Materials, College of Chemistry
Beijing Normal University
No. 19, XinJieKouWai Street, Beijing, 100875 (China)
E-mail: dongyq@bnu.edu.cn
[b] Dr. H. Ma, Dr. Q. Peng
Key Laboratory of Organic Solids, Beijing National Laboratory for Molecular Science
Institute of Chemistry, Chinese Academy of Sciences
Beijing, 100190 (China)

Supporting information and the ORCID identification number(s) for the author(s) for this article is given via a link at the end of the document.

nm. All the four aggregates exhibit enhanced emission intensity at lower temperature, but only the orange emissive crystals exhibit blue-shifted emission. The emission of **1** can be switched reversibly between any two of the four states by mechanical, solvent vapor, and thermal treatment. The potential application of **1** in optical data storage was also investigated.

Results and Discussion

Luminogen **1** was synthesized according to the synthetic route given in Scheme 1. Detailed synthetic methods and structural characterization of the product are described in the Supporting Information.

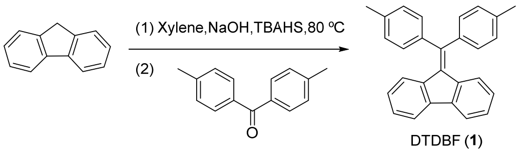

Scheme 1. Synthetic route to DTDBF (**1**).

Similar to other diphenyldibenzofulvene derivatives, luminogen **1** is also AIE active. As indicated by the PL spectrum and photo in Figure S1, luminogen **1** is nearly nonemissive when molecularly dissolved in acetonitrile. However, the emission of **1** is turned on when a large amount of water was added to the solution. As is shown in Figure S1, luminogen **1** emits orange light in acetonitrile/water mixtures and emission intensity gradually increased when the volume fraction of water increased from 70% to 90%. The addition of large volume of water causes aggregation of molecules of **1** as water is a nonsolvent of **1**, that is, luminogen **1** is AIE active.

In addition to the suspension of luminogens, the optical properties of luminogens in the solid state deserve more attention as many luminogens are used in the solid state in real application. Many AIEgens exhibit morphology dependent emission, and disclosure of the relation between morphology and optical properties will facilitate molecular design of high performance luminogens. Single crystal XRD can provide detailed molecular information in crystals. The availability of different single crystals of one luminogen will eliminate the effect of molecular structure, and may be the key point to study the effect of molecular conformation, packing patterns, and interactions on its optical properties. Then we tried to grow single crystals of **1** through slow evaporation of organic solvents from the solution of **1** at room temperature. Fortunately, three single crystals with varied emission colors and efficiencies were obtained: orange emissive column-like crystals (**1**CO, Figure 1a, emitting at 586 nm, Φ_F = 16.2%) were obtained by slow evaporation of a chloroform/hexane solution, yellow emissive needle-like crystals (**1**CY, Figure 1c, emitting at 545 nm, Φ_F = 23.3%) were from acetone/ethanol solution, and blue emissive crystals (**1**CB, in block shape, Figure 1d, emitting at 460 nm, Φ_F = 28.1%) were from dichloroethane (DCE) /ethanol solution. Besides the visual evidence and PL spectra, differential scanning calorimetry (DSC) curves (Figure 1f) and powder XRD patterns (Figure 1g) of 1CO, 1CY, 1CB also revealed their different morphology.

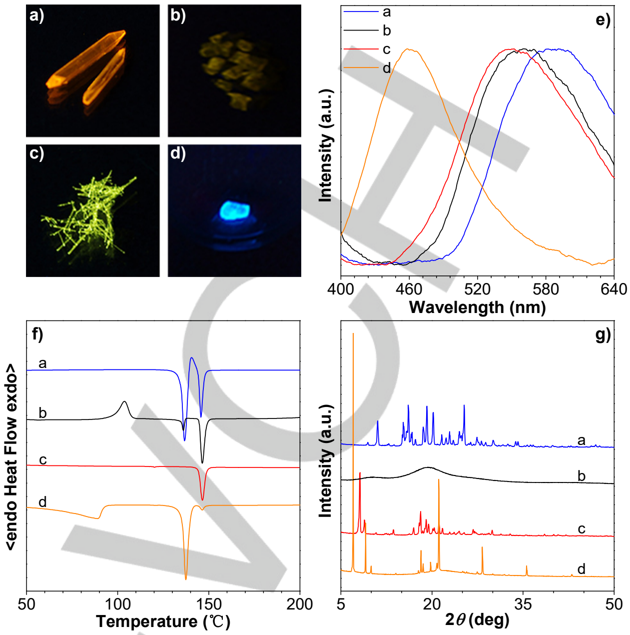

Figure 1. Photos of (a) **1**CO, (b) **1**Am, (c) **1**CY, (d) **1**CB, (e) PL spectra (Excitation wavelength: 360 nm), (f) DSC curves, (g) powder XRD patterns of samples (a)−(d) in the images. Photos were taken under UV illumination.

In addition to its crystalline phases, the amorphous solid of **1** (**1**Am) were obtained through quenching of its melt, and its amorphous essence is verified by the crystalline peak in the DSC curve (line b in Figure 1f) and the absence of sharp diffraction peak in the powder XRD pattern (line b in Figure 1g). **1**Am emit weak orange light peaking at 557 nm with efficiency of 2.9%, which is much lower than its crystalline cousins, that is, luminogen **1** is CIEE active. Thus, it is clear that luminogen **1** exhibits tetracolored emissions with high contrast in both emission color (586, 557, 545, 461 nm) and emission efficiency (16.2, 2.9, 23.3, 28.1%) depending on its morphology, which is seldom reported.

The optical properties of the four morphologies of **1** were summarized in Table 1.

To disclose the origin of varied optical properties of different crystalline phases of 1, we carefully checked the molecular conformations, packing patterns, and interactions in the three crystalline phases. Specific strong intermolecular interactions (such as π – π stacking or H/J-aggregates) were ruled out due to the twisted molecular conformations in all the crystals of 1. Thus, the emissions of crystals of 1 should be from single molecule which mainly depends on the molecular conformation.

The dibenzofulvene part of molecule of **1** is inflexible, thus, its conformation depends on the torsion angles (θ_1 and θ_2) between two phenyl rings and the double bond. Examination of the conformation of **1** in single crystals revealed that the torsion angles of two phenyl rings increase in the sequence of **1**CO (50.51, 47.26), **1**CY (68.77, 60.41) and **1**CB (88.22, 85.14) (Table S1) indicating that the planarity of **1** decrease in the order of **1**CO, **1**CY and **1**CB. Thus, the conjugation degree of molecules of **1** decreases in the sequence of **1**CO, **1**CY and **1**CB, hence emission of **1** blue-shift from 585 nm (**1**CO) to 546 nm (**1**CY) and 461 nm (**1**CB). Then it is clear that the emission colors of crystals of **1** fit well with their conformation.

Amorphous solid of many CIEE active luminogens exhibit redder emission in comparison with their crystalline phases, while emission of **1**Am falls between two crystalline phase of **1**CO and **1**CY. As molecules adopt random conformations and pack accidentally in amorphous solid, the detailed conformation and packing pattern cannot be obtained through experimental method. Thus, we speculated that the average torsion angle of molecules in **1**Am may be between those of **1**CO and **1**CY.

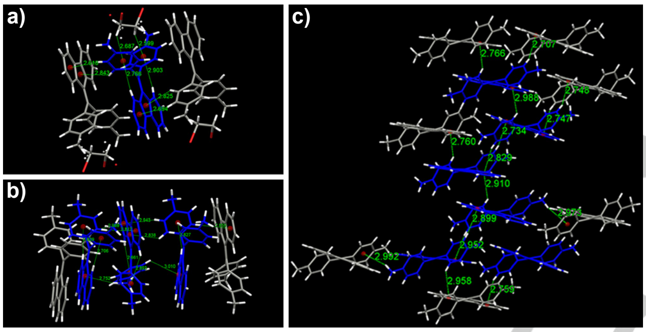

Figure 2. Analysis of the C-H···π interactions (green line) in single crystal structures of (a) **1**CB, (b) **1**CY, (c) **1**CO.

Table 1. Optical Properties of Luminogen **1** in Varied Aggregate States Table Caption. ((**Note:** Please do **not** include the table in a textbox or frame))

1	λ_{em}[a] (nm)	Φ_F[b] (%)	fluorescence decay A1/A2[c]	τ1 (ns)	τ2 (ns)	⟨τ⟩[d] (ns)
1CO	586	16.2	100/0	1.7		1.7
1CY	545	23.3	100/0	2.9		2.9
1CB	461	28.1	100/0	39.2		39.2
1Am	557	2.9	80/20	0.9	1.9	1.1

[a] λ_{em} = emission maximum. [b] Φ_F = fluorescence quantum yield determined using a calibrated integrating sphere, excited at 340 nm. [c] Fraction (A, %) and lifetime (τ, ns) of shorter (1) or longer lived species (2). [d] The mean lifetime ⟨τ⟩ was calculated according to $\langle\tau\rangle = (A_1\tau_1 + A_2\tau_2)/(A_1 + A_2)$.

In addition to the morphology dependent emission color, luminogen **1** also exhibits high contrast emission efficiency relying on its morphology. The quantum yield of **1**CB, **1**CY, **1**CO and **1**Am was 28.1, 23.3, 16.2 and 2.9%, respectively. Disclosure of the cause of the morphology dependent emission efficiency may facilitate the molecular design of high efficiency luminogens. As aforementioned, no strong intermolecular interactions (such as π – π stacking or H/J-aggregates) were found in the three single crystals. Then we checked the weak interaction of C−H•••π in the three single crystals. The asymmetric units of **1**CB, **1**CY, **1**CO contain one, three, and six molecules of **1**, which is marked in blue color in the crystal structure image (Figure 2). In the asymmetric unit of **1**CB, the conformation of one molecule was solidified by eight C−H•••π interactions. However, in the asymmetric units of **1**CY and **1**CO, the numbers of C−H•••π interaction is twelve for three molecules and fifteen for six molecules, respectively. Then, it is clear that the emission efficiencies of difference crystalline phases depend on the average number of C−H•••π interactions per molecule. More interactions help to solidify the molecular conformation more tightly and block the non-radioactive pathways, and then increase the emission efficiency. Compared with the crystals of **1**, the emission efficiency of **1**Am is lowered to 2.9%, which may be attributed to the loose packing pattern and less rotation restriction in amorphous solid or energy transfer to the emission species with low quantum yield. Following this line, high efficiency luminogens may be generated through introduction of groups exhibiting strong interactions to the twisted conjugation core.

In addition to the steady-state spectra measurements, time-resolved PL spectra of the four morphologies of **1** were measured and the dynamic parameters are summarized in Table 1. All the three crystals display monoexponential PL decays with long lifetime, indicating single decay mechanism, and **1**CB exhibit ultra-long fluorescence lifetime of 39.2 ns. The lifetime increases promptly with the number of C−H•••π interaction, which coincides well with the increase of PL efficiency. Emission of **1**Am decay bi-exponentially with 80% of short component and 20% long component, suggesting the availability of quick decay process due to the loose packing pattern in the amorphous solid.

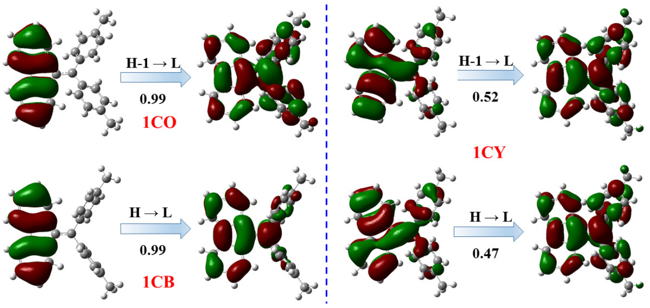

Figure 3. Calculated transition molecular orbitals of the lowest singlets states S1 at S1-geometry for **1**CO, **1**CY and **1**CB.

To gain deeper insight on the luminescent properties of these different crystalline phases of **1**, theoretical computations are performed to probe the excited state electronic structure at (TD)B3LYP/6-31G(d) level as shown in Table S2. From **1**CO, **1**CY to **1**CB, the calculated emission peaks are blue-shifted from

582, 562 to 464 nm, which well reproduced the experimental results (585, 546 and 461 nm for **1**CO, **1**CY and **1**CB, respectively). This is because the lowest singlet state S1 of **1**CY is consist of local excitation and charge transfer transition. When going to **1**CB, the S1 state is dominated by local excitation (see Figure 3.), and hence leads to blue-shift emission. It is known that the non-radiative rate k_{nr} is the crucial factor for the luminescent property of AIE systems, while the reorganization energy is responsible for the k_{nr}.[17] Table S2 shows that the **1**CY and **1**CO have the same reorganization energy 0.49 eV, and it reduces to 0.43 eV for **1**CB, which will result in a slower non-radiative rate. Therefore, **1**CB possess high quantum yield and long fluorescent lifetime in comparison with **1**CY and **1**CO.

In addition to morphology dependent emission, we noticed that some AIEgens exhibit temperature dependent emission color. Although some luminogens solutions have been reported to exhibit increased emission efficiency and blue-shifted emission color at low temperature, temperature dependent emission of solid luminogens have seldom been reported. The availability of four morphologies of **1** provides us the opportunity to study the effect of molecular conformation and interaction on the temperature dependent emission avoiding the influence of molecular structure and complex solvent environment.

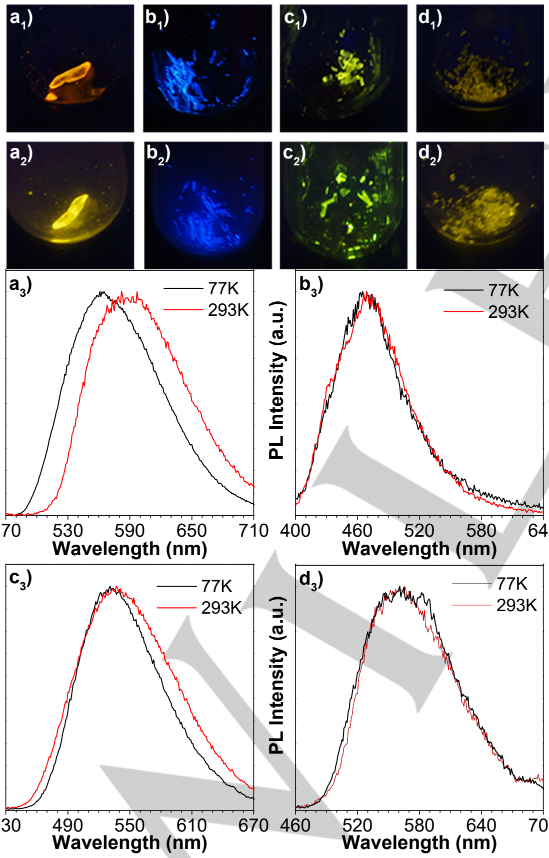

Figure 4. Photos of (a_1,a_2) **1**CO before and after freeing, (b_1,b_2) **1**CB before and after freeing, (c_1,c_2) **1**CY before and after freeing, (d_1,d_2) **1**Am before and after freeing. (a_3-d_3) PL spectra of (a_3) **1**CO, (b_3) **1**CB, (c_3) **1**CY, (d_3) **1**Am before and after freezing. Excitation wavelength: 360 nm. Photos were taken under UV illumination.

All the morphologies of luminogen **1** exhibit greatly increased emission intensity at lower temperature compared with room temperature. Emission color and PL spectra of **1**CB, **1**CY and **1**Am at 77 K fit well with those at room temperature (Figure 4). However, emission of **1**CO transferred from orange to yellow with 25 nm blue-shift of PL spectrum in response to freezing with liquid nitrogen. The large amplitude geometric change in excited state may be blocked at low temperature, thus, the emissions of luminogens should blue-shifted compared with those at room temperature. However, why only **1**CO exhibit blue-shifted emission? As aforementioned, compared with **1**CO, there are more C−H•••π interactions in **1**CB and **1**CY, which have already prevented the large amplitude conformation relaxation at room temperature. Hence **1**CB and **1**CY exhibit no emission color change upon freezing. As a result of less C−H•••π interactions, molecules in **1**CO may exhibit large amplitude geometric change at room temperature, which may be forbidden at low temperature. **1**Am also exhibit no emission color change upon freezing due to the loose packing pattern in amorphous solid, as the large amplitude vibrational relaxation may not be restricted even at 77K.

Luminogen **1** exhibits tetracolored emissions with high contrast depending on its morphology, thus, its emission may be modulated through morphology tuning. As aforementioned, **1**Am can be obtained through quenching of the melt of **1**, then, emissions of all the three crystals can be turned to dark orange through heating to melt and quenched with liquid nitrogen quickly.

Amorphous solids will crystallize under organic solvent atmosphere. Thus, we tried to fume **1**Am (Figure 5a) with DCE and acetone vapor and the emission of the amorphous solid turned to blue (Figure 5b) and orange (Figure 5c), respectively. In addition to the visual evidence, the PL spectra, DSC curves and powder XRD patterns (line b and c in Figure 5) of the fumed solid fit well with those of **1**CB (line d in Figure 1) and **1**CO (line a in Figure 1), respectively, indicating their same crystalline essence. In addition to solvent fuming, the exothermic peak at 110 °C and endothermic peak at 138 °C in the DSC curve of **1**Am suggest availability of two phase transitions, and then **1**Am could transform to **1**CO (Figure 5a to 5d) when heat at 110 °C and the obtained **1**CO can transform to **1**CY (Figure 5d to 5e) when further heated at 138 °C. **1**Am can also be converted to **1**CY directly upon heating at 138 °C (Figure 5a to 5f). Then it is clear that emission of **1** can be tuned from dark orange (**1**Am) to bright blue (**1**CB), yellow (**1**CY) or orange (**1**CO) through tuning solid of **1** between disordered (amorphous) and three ordered (crystalline) morphologies.

In addition to morphology tuning between amorphous and crystalline, we try to modulate luminogen **1** among the three crystalline states. The endothermic peak at 138 °C in the DSC curve of **1**CO suggests a phase transformation, thus, we heated **1**CO at 138 °C for ten minutes and the orange emissive **1**CO turned to yellow emissive solid (Figure 5j to 5k). The PL spectrum, DSC curve, and powder XRD pattern of the heated sample fit well with those of **1**CY, suggesting that **1**CO had transform to **1**CY upon heating. Furthermore, **1**CY can also be converted to **1**CO upon fuming with acetone (Figure 5k to 5l), thus, the transformation between **1**CY and **1**CO is reversible and can be repeated many times (Figure S2a). Both **1**CO and **1**CY can be transfer to blue emissive crystals (Figure 5j to 5m and Figure 5o to 5p) upon fuming with DCE. The PL spectrum, DSC curve and powder XRD pattern of the obtained blue emissive crystals fit well with those of **1**CB, verifying that **1**CB could be obtained through fuming **1**CO or **1**CY with DCE. And **1**CB can transform back to **1**CO (Figure 5m to 5n) upon fuming with acetone or heating at 100 °C, but to **1**CY upon heating at 130 °C. (Figure 5p to 5q) Similarly, transformation between **1**CO and **1**CB (Figure S2b) and transformation between **1**CY and **1**CB (Figure S2c) are reversible and can be repeated many times. Then, it is clear that we can reversibly switch luminogen **1** among three different crystalline states. Together with **1**Am, emission of **1** can be reversibly tuned among four different states with high contrast in both emission color and efficiency through morphology modulation, which is seldom reported.

The distinctive polymorph-dependent emission property of luminogen **1** inspires us to study its MC luminescence. All the three crystals can be converted to dark orange emissive solid upon grinding, whose PL spectrum match well with that of **1**Am. The DSC curve of the ground solid exhibit exothermic peak at 75 °C (line a in Figure S3g), and its powder XRD pattern shows nearly no diffraction peaks (line a in Figure S4h), indicating the amorphous essence of the ground solid. Similar to **1**Am, the ground solid transformed to **1**CO upon heating at 75 °C or fumed with acetone, which is verified by coincidence of its PL spectrum, DSC curve and powder XRD pattern with those of **1**CO. And the ground solid can also be converted to **1**CY directly upon heating at 138 °C. **1**CY and **1**CO obtained from treating the ground solid behave similarly to those obtained from solvent evaporation. The ground solid can also transform to blue emissive powder upon fuming with DCE, while the fumed sample reverted back to its original morphology quickly.

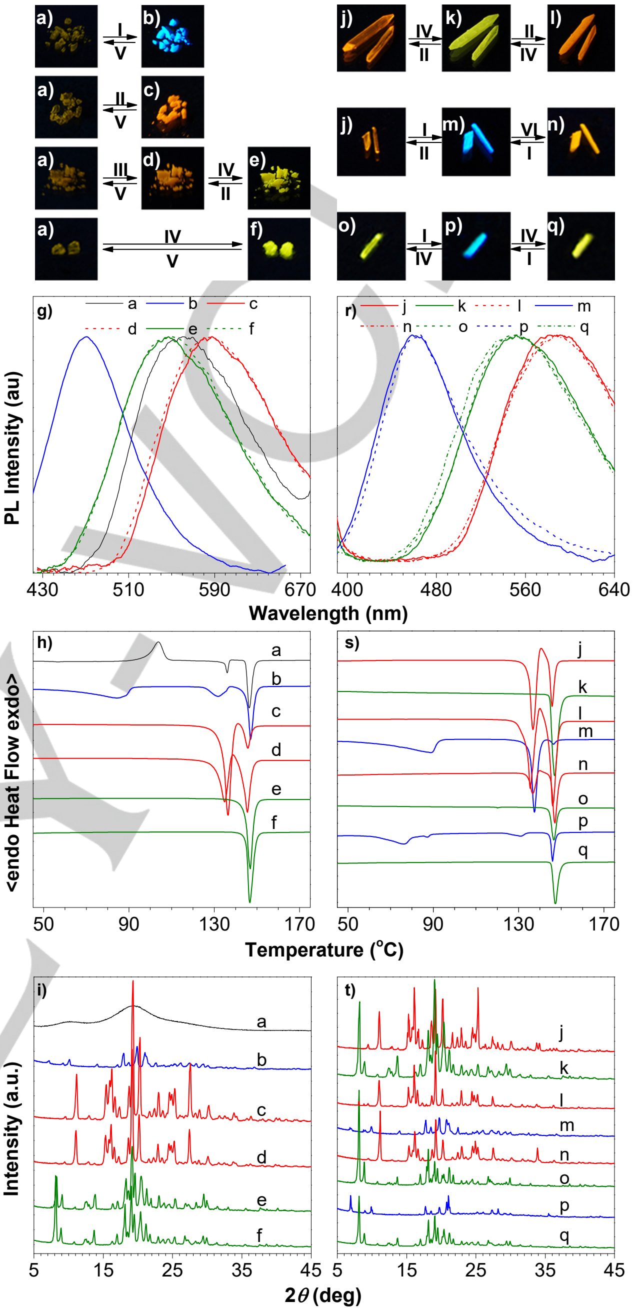

Figure 5. Photos of (a) **1**Am, (b) **1**Am fumed by DCE, (c) **1**Am fumed by acetone, (d) **1**Am annealed at 110 °C, (e) d annealed at 135 °C, (f) **1**Am annealed at 138 °C. (g) PL spectra. Excitation wavelength: 360 nm. (h) DSC curves. (i) powder XRD patterns of samples (a)−(f) in the images. (j) **1**CO, (k) **1**CO annealed at 138 °C, (l) k fumed by acetone, (m) **1**CO fumed by DCE vapor. (n) m annealed at 130 °C, (o) **1**CY, (p) **1**CY fumed by DCE, (q) p annealed at 138 °C. (r) PL spectra. Excitation wavelength: 360 nm. (s) DSC curves. (t) powder XRD patterns of samples (j)−(q) in the images. Photos were taken under UV illumination. Conditions: I, fuming with DCE vapor; II, fuming with acetone vapor; III, 110°C, 10 min; IV, 138 °C, 10 min; V, heating to melt and cooling quickly; VI, 130 °C, 10 min.

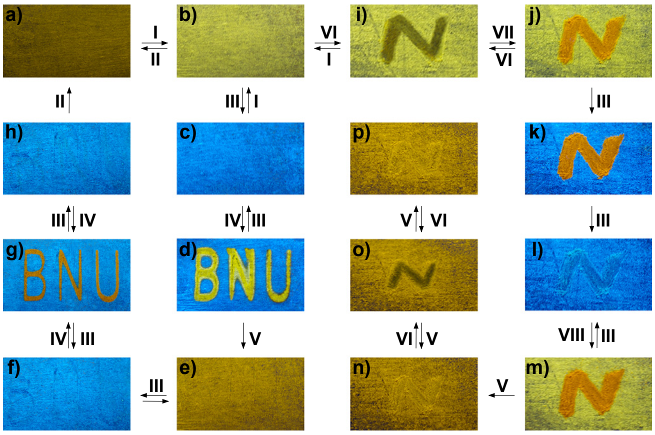

Figure 6. Application of luminogen 1 in optical recording. Conditions: I, 138 °C, 10 min; II, grinding; III, fuming with DCE vapor; IV, heating with a hot stamp of 130 °C; V, fuming with acetone vapor; VI, writing with a glass bar; VII, 75 °C, 10 min; VIII, 130 °C, 10 min.

The multicolored morphology dependent fluorescence of **1** prompts us to investigate its potential application in optical recording. Luminogen **1** was ground on a piece of weighing paper, and a dark orange emissive paper was obtained (Figure 6a). The dark orange emissive paper turned to yellow when heated at 130 °C (Figure 6b) due to the transformation from **1**Am to **1**CY. The yellow emissive paper can be turned blue emissive (Figure 6c) upon fuming with DCE vapor due to the transformation from **1**CY to **1**CB. Then we put a hot stamp of 130 °C on the blue emissive paper, a yellow emissive "BNU" appeared on the blue background (Figure 6d) due to the transformation of luminogen **1** from **1**CB to **1**CY in the heating area. The letter could be erased upon fuming with acetone vapor and an orange emissive paper was obtained (Figure 6e) as both blue (**1**CB) and yellow (**1**CY) emissive luminogen on the paper could transform to **1**CO under acetone atmosphere. The orange emissive paper could turned to blue (Figure 6f) upon fuming with DCE vapor as luminogen **1** transform from **1**CO to **1**CB. When the blue emissive paper was treated with the a hot stamp of 130 °C, an orange emissive "BNU" appeared on the blue background (Figure 6g) due to the transformation from **1**CB to **1**CO in the heating area. Similarly, the letter could be erased through fuming with DCE (Figure 6h). Then it is clear that, the blue emissive paper can remember its origin: the one from yellow emissive paper converted back to yellow upon heating, while the one from orange reverted back to orange upon heating. Trace amount of original crystals may exist in 1CB obtained from fuming 1CY or 1CO, which may serve as seed crystal and induced the 1CB transform back to its original crystalline state upon heating.

In addition to thermal recording, mechanical method is also effective. When we wrote "N" on the yellow emissive paper (Figure 6b) with a glass rod, a dark orange letter appeared on the yellow backgrounds due to the amorphization of **1** in the written area (Figure 6i). When the paper was heated at 75 °C, the "N" turned to orange (Figure 6j) due to the transformation from **1**Am to **1**CO, while the yellow emissive background remained unchanged as **1**CY is stable at this temperature.

The yellow background turned to blue but the orange letter remained unchanged (Figure 6k) upon fuming with DCE for 5 min. The letter could be erased upon further fuming with DCE vapor up to 10 min, and a blue emissive paper (Figure 6l) was obtained due to the transformation of **1** from **1**CO to **1**CB. This process was controlled by the fuming time, as **1**CY transfer to **1**CB more quickly than **1**CO does upon fuming.

Interestingly, the optical information of Figure 6j appeared again when heating the blue paper at 130 °C (Figure 6m). As aforementioned, **1**CB obtained from **1**CY or **1**CO can revert back to its original crystalline phase, thus, **1**CB in the letter area turn back to **1**CO, and the background turn back to yellow (**1**CY). The letter was erased upon fuming with acetone and an orange emissive paper was obtained (Figure 6n) due to the transformation of **1** in the background area from **1**CY to **1**CO. When we wrote "N" on the orange emissive paper (Figure 6b) with a glass bar, a dark orange letter appeared on the orange backgrounds (Figure 6o) due to the amorphization of **1** in the written area. The letter could be erased upon fuming the paper with acetone vapor (Figure 6p) due to the transformation of **1** in the letter area from **1**Am to **1**CO.

Conclusions

In conclusion, we construct a luminogen through combination of bulky conjugation core and peripheral phenyl rings. The luminogen can form four morphologies including three crystalline phases and the amorphous state, which exhibits high contrast in both emission color and efficiency. The high contrast in the emission can be attributed to the variance in torsion angle of phenyl rings, and larger torsion angle induces bluer emission. The efficiency difference of the four morphologies is caused by different number of the weak interaction among molecules, and more interactions on per molecule induces higher emission efficiency. The multi-colored emission switching affords its potential application in optical recording and anti-faking.

Experimental Section

Experimental Details can be found in the ESI. CCDC number for single crystals of 1CO, 1CY, and 1CB are 1876225, 1502860, 1502858, respectively.

Computational details

The computational models were built from X-ray diffractions crystal structure as shown in Figure S5. The quantum mechanics/molecular mechanics (QM/MM) with two-layer ONIOM method was implemented to deal with the electronic structures in crystal by using the universal force field (UFF) for MM part. The electronic embedding are adopted in QM/MM calculations by incorporating the partial charges of the MM region into the quantum mechanical Hamiltonian. The atomic partial charges were generated by the restrained electrostatic potential (RESP)[18] method. Molecular geometry optimizations were performed for the ground state (S_0) at the level of B3LYP/6-31G(d) and for the singlet state (S_1) at the TDDFT/B3LYP/6-31G(d) level. The excitation energies were calculated by using

TDDFT for electronic excited singlet states. All the calculations were carried out by using Gaussian 09 program.[2]

Acknowledgements

This work was partially supported by the National Science Foundation of China (51773020, 51173018), the Fundamental Research Funds for the Central Universities, and Program for Changjiang Scholars and Innovative Research Team in University.

Keywords: • AIE • fluorescence • sensor • mechanochromic luminescence • stimuli responsive luminogen

[1] a) A. Kishimura, T. Yamashita, K. Yamaguchi, T. Aida, *Nat. Mater.* **2005**, *4*, 546-549; b) S. Hirata, T. Watanabe, *Adv. Mater.* **2006**, *18*, 2725-2729; c) Y. Dong, J. W. Y. Lam, A. Qin, Z. Li, J. Sun, H. H. Y. Sung, I. D. Williams, B. Z. Tang, *Chem. Commun.* **2007**, 40-42; d) J. Yang, X. Zhen, B. Wang, X. Gao, Z. Ren, J. Wang, Y. Xie, J. Li, Q. Peng, K. Pu, Z. Li, *Nat. Commun.* **2018**, *9*; e) Z. Wang, X. Cheng, A. Qin, H. Zhang, J. Z. Sun, B. Z. Tang, *J. Phys. Chem. B* **2018**, *122*, 2165-2176; f) T. Hu, B. Yao, X. Chen, W. Li, Z. Song, A. Qin, J. Z. Sun, B. Z. Tang, *Chem. Commun.* **2015**, *51*, 8849-8852.

[2] a) Y. Sagara, T. Kato, *Nat. Chem.* **2009**, *1*, 605-610; b) Z. Chi, X. Zhang, B. Xu, X. Zhou, C. Ma, Y. Zhang, S. Liu, J. Xu, *Chem. Soc. Rev.* **2012**, *41*, 3878-3896; c) Z. Yang, Z. Chi, Z. Mao, Y. Zhang, S. Liu, J. Zhao, M. P. Aldred, Z. Chi, *Mater. Chem. Front.* **2018**, *2*, 861-890; d) W. Z. Yuan, Y. Tan, Y. Gong, P. Lu, J. W. Y. Lam, X. Y. Shen, C. Feng, H. H. Y. Sung, Y. Lu, I. D. Williams, J. Z. Sun, Y. Zhang, B. Z. Tang, *Adv. Mater.* **2013**, *25*, 2837-2843; e) Y.-B. Gong, P. Zhang, Y.-r. Gu, J.-Q. Wang, M.-M. Han, C. Chen, X.-J. Zhan, Z.-L. Xie, B. Zou, Q. Peng, Z.-G. Chi, Z. Li, *Adv. Optical Mater.* **2018**, *6*.

[3] Y. Sagara, T. Kato, *Angew. Chem. Int. Ed.* **2011**, *50*, 9128-9132.

[4] S.-J. Yoon, J. W. Chung, J. Gierschner, K. S. Kim, M.-G. Choi, D. Kim, S. Y. Park, *J. Am. Chem. Soc.* **2010**, *132*, 13675-13683.

[5] X. Zhang, Z. Chi, Y. Zhang, S. Liu, J. Xu, *J. Mater. Chem. C* **2013**, *1*, 3376-3390.

[6] A. Pucci, G. Ruggeri, *J. Mater. Chem.* **2011**, *21*, 8282.

[7] Y. Hong, J. W. Y. Lam, B. Z. Tang, *Chem. Commun.* **2009**, 4332-4353.

[8] J. D. Luo, Z. L. Xie, J. W. Y. Lam, L. Cheng, H. Y. Chen, C. F. Qiu, H. S. Kwok, X. W. Zhan, Y. Q. Liu, D. B. Zhu, B. Z. Tang, *Chem. Commun.* **2001**, 1740-1741.

[9] Y. Q. Dong, J. W. Y. Lam, Z. Li, A. J. Qin, H. Tong, Y. P. Dong, X. D. Feng, B. Z. Tang, *J. Inorg. Organomet. Polym. Mater.* **2005**, *15*, 287-291.

[10] Y. Q. Dong, J. W. Y. Lam, B. Z. Tang, *J. Phys. Chem. Lett.* **2015**, *6*, 3429-3436.

[11] a) X. Luo, W. Zhao, J. Shi, C. Li, Z. Liu, Z. Bo, Y. Q. Dong, B. Z. Tang, *J. Phys. Chem. C* **2012**, *116*, 21967-21972; b) W. Zhao, Z. He, Q. Peng, J. W. Y. Lam, H. Ma, Z. Qiu, Y. Chen, Z. Zhao, Z. Shuai, Y. Dong, B. Z. Tang, *Nat. Commun.* **2018**, *9*, 3044; c) Y. Gong, Y. Zhang, W. Z. Yuan, J. Z. Sun, Y. Zhang, *J. Phys. Chem. C* **2014**, *118*, 10998-11005.

[12] Y. Zhang, K. Wang, G. Zhuang, Z. Xie, C. Zhang, F. Cao, G. Pan, H. Chen, B. Zou, Y. Ma, *Chem.-Eur. J.* **2015**, *21*, 2474-2479.

[13] Z. Ma, Z. Wang, X. Meng, Z. Ma, Z. Xu, Y. Ma, X. Jia, *Angew. Chem. Int. Ed.* **2016**, *55*, 519-522.

[14] C. Ma, B. Xu, G. Xie, J. He, X. Zhou, B. Peng, L. Jiang, B. Xu, W. Tian, Z. Chi, S. Liu, Y. Zhang, J. Xu, *Chem. Commun.* **2014**, *50*, 7374-7377.

[15] Y. Sagara, A. Lavrenova, A. Crochet, Y. C. Simon, K. M. Fromm, C. Weder, *Chem. Eur. J.* **2016**, *22*, 4374-4378.

[16] a) X. L. Luo, J. N. Li, C. H. Li, L. P. Heng, Y. Q. Dong, Z. P. Liu, Z. S. Bo, B. Z. Tang, *Adv. Mater.* **2011**, *23*, 3261-3265; b) Z. Zhao, T. Chen, S. Jiang, Z. Liu, D. Fang, Y. Q. Dong, *J. Mater. Chem. C* **2016**, *4*, 4800-4804.

[17] a) Y. Niu, Q. Peng, C. Deng, X. Gao, Z. Shuai, *J. Phys. Chem. A* **2010**, *114*, 7817-7831; b) Z. Shuai, Q. Peng, *Phys. Rep.* **2014**, *537*, 123-156.

[18] C. I. Bayly, P. Cieplak, W. D. Cornell, P. A. Kollman, *J. Phys. Chem.* **1993**, *97*, 10269-10280.

[19] M. J. Frisch, G. W. Trucks, H. B. Schlegel, G. E. Scuseria, M. A. Robb, J. R. Cheeseman, G. Scalmani, V. Barone, B. Mennucci, G. A. Petersson, H. Nakatsuji, M. Caricato, X. Li, H. P. Hratchian, A. F. Izmaylov, J. Bloino, G. Zheng, J. L. Sonnenberg, M. Hada, M. Ehara, K. Toyota, R. Fukuda, J. Hasegawa, M. Ishida, T. Nakajima, Y. Honda, O. Kitao, H. Nakai, T. Vreven, J. A. Montgomery, Jr., J. E. Peralta, F. Ogliaro, M. Bearpark, J. J. Heyd, E. Brothers, K. N. Kudin, V. N. Staroverov, T. Keith, R. Kobayashi, J. Normand, K. Raghavachari, A. Rendell, J. C. Burant, S. S. Iyengar, J. Tomasi, M. Cossi, N. Rega, J. M. Millam, M. Klene, J. E. Knox, J. B. Cross, V. Bakken, C. Adamo, J. Jaramillo, R. Gomperts, R. E. Stratmann, O. Yazyev, A. J. Austin, R. Cammi, C. Pomelli, J. W. Ochterski, R. L. Martin, K. Morokuma, V. G. Zakrzewski, G. A. Voth, P. Salvador, J. J. Dannenberg, S. Dapprich, A. D. Daniels, O. Farkas, J. B. Foresman, J. V. Ortiz, J. Cioslowski and D. J. Fox, Gaussian 09, Revision E.01. Gaussian, Inc.: Wallingford CT, 2013.

Entry for the Table of Contents (Please choose one layout)

FULL PAPER

Emission of ditolyldibenzofulvene can be reversibly switched among four different states with high contrast through morphology modulation by solvent fuming, heating, and mechanical stimuli.

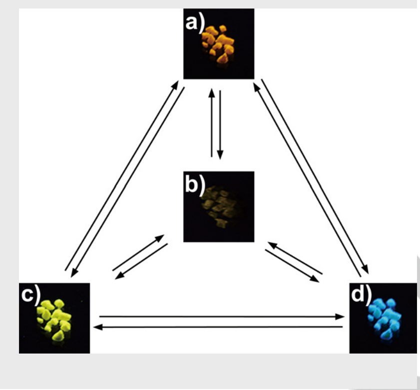

Yuxin Duan, [a] *Dr. Huili Ma,* [b] *Haiyan Tian,* [a] *Jing Liu,* [a] *Xuebin Deng,* [a] *Dr. Qian Peng,* *[b] *and Yong Qiang Dong,** [a]

Page No. – Page No.

Construction of a Luminogen Exhibiting High Contrast and Multicolored Emission Switching through Combination of a Bulky Conjugation Core and Tolyl Groups